Available online at www.sciencedirect.com

ScienceDirect

Procedia Manufacturing 13 (2017) 36–42

Procedia MANUFACTURING

www.elsevier.com/locate/procedia

Manufacturing Engineering Society International Conference 2017, MESIC 2017, 28-30 June 2017, Vigo (Pontevedra), Spain

Numerical modeling of instabilities during machining of aeronautical alloy

X. Soldani[a,]*, H. López-Gálvez[a], J. Díaz-Álvarez[b]

[a]*Department of Mechanical Engineering, Universidad Carlos III de Madrid, Avda. de la Universidad 30, Leganés 28911, Spain.*
xsoldani@ing.uc3m.es
[b]*Department of Bio-Engineering and Aerospacial Engineering*

Abstract

Machining processes induce high strain, strain rate and temperature in the machined material. Into model such thermodynamic chip removal process a good description of the material behavior is needed. In this paper is proposed a parametrical study to determine the fracture energy of Ti6Al4V during its machining. The effect of the fracture energy on the cutting forces and the chip morphology is presented and compared with experimental tests of orthogonal cutting to validate the numerical model.

Peer-review under responsibility of the scientific committee of the Manufacturing Engineering Society International Conference 2017.

Keywords: Machining ; Numerical Model ; Ti6Al4V Alloy ; Damage

1. Introduction

Manufacturing by machining process such as milling or turning is not only, one of the most common industrial process, but also a complex process due its dynamic and thermo-mechanical nature [1]. Experimental investigations on cutting forces, temperatures, chip morphology or surface roughness are essential information which allow to understand the chip formation process, the tribological phenomenon [2], the tool wear or the residual stress induced in the machined workpiece [3, 4].

The Finite Element (FE) models have been widely used in the last decades to simulate and understand the chip formation processes, to predict cutting forces [5, 6], the distribution of temperature on the tool rake face [7] or the residual stresses in the machined material [8]. Two-dimensional models have been used to simulate orthogonal cutting process. S. Atlati et al. [1] studied in 2004 the tribological effects on shear band apparition in dry machining. The shear band phenomenon has been also deeply studied by M. Calamaz et al. [9], M.H. Miguélez et al. [10] or A.

2351-9789
Peer-review under responsibility of the scientific committee of the Manufacturing Engineering Society International Conference 2017.
10.1016/j.promfg.2017.09.006

Molinari et al. [11]. In order to achieve a good understanding of machining processes through FE models, the damage criteria and its calibration has a capital importance.

The paper is focused on the numerical investigation of chip segmentation of an aeronautical alloy (Ti6Al4V) during its machining. Ti alloys are widely used for high performance components in sectors such as the aeronautical or bio-medical; its manufacturability is therefore a crucial investigation field. Chip removal processes of Ti alloys induce to the machined material very high levels of strain, strain rate and temperature inducing differences in the obtained chip morphologies. Serrated and segmented chips are the result of the competition between stabilizing (strain and strain rate hardening) and destabilizing effects (thermal softening) [10].

The objective of this work is to develop a numerical model of machining taking into account the damage of the material. The energy of fracture of the machined material was numerically studied to investigate its effect on the cutting forces and chip segmentation.

2. Numerical model

The two dimensional numerical model of orthogonal cutting was developed with the commercial finite element code ABAQUS/Explicit. Geometry and boundary conditions are presented in Fig. 1 (the tool rake angle, the incidence angle, the feed and the width of cut are respectively $\alpha = 0°$, $\beta = 7°$, $t_1 = 0.1$ mm and $p = 1$ mm).

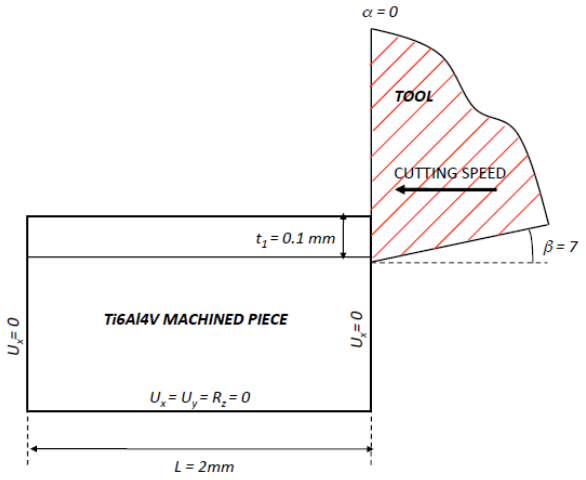

Fig. 1. Geometry and boundary conditions of the orthogonal cutting model proposed.

2.1. Ti6Al4V mechanical and thermal properties.

The machined material was taken to be isotropic, elasto-viscoplastic, and to obey to the J_2 flow theory (von Mises yield criterion). Into describe the material behaviour, the Johnson-Cook phenomenological law has been chosen [12]

$$\sigma = \left(A + B\varepsilon_p^n\right)\left(1 + C ln\frac{\dot{\varepsilon_p}}{\dot{\varepsilon_0}}\right)\left(1 - \left(\frac{T-T_0}{T_m-T_0}\right)^m\right) \quad (1)$$

with σ the tensile flow stress, ε_p the plastic strain, $\dot{\varepsilon_p}$ the equivalent plastic strain rate and T the absolute temperature (T_0 and T_m represent respectively the room and the melting temperature of the material – T_m = 1673 K). The constitutive law parameters (A, B, n, c and m) have been determined by [3] for a referential strain rate $\dot{\varepsilon_0}$=1 x 10^{-5} and are resumed in Table 1. The thermal and mechanical parameters of Ti6Al4V used in the numerical model are shown in Table 2.

Table 1: Jonson-Cook parameters for Ti6Al4V alloy [13].

A (Mpa)	B (Mpa)	n	c	m
782	498	0.28	0.028	1

Table 2: Thermal and mechanical parameters for Ti6Al4V [10].

Ti6Al4V	
Thermal Conductivity - 293 K - (W/m/K)	7
Specificic Heat Capacity (J/Kg/K)	560
Thermal Expansion (/K)	9.2 x 10-6
Density (kg/m3)	4.42
Poisson Ratio	0.3
Modulus of Elasticity (Gpa)	114

2.2. Heat transfer and tool/chip interaction

In machining, heat generation has two contributions: plastic work and the friction at the tool/chip interface. Concerning plastic work, the value of the Quinney-Taylor coefficient is taken equal to $\beta=0.92$. The initial temperature T_0 for the tool and the workpiece is equal to *293 K*, the melting temperature of Ti6Al4V is *1573 K*.

The contact at the tool/chip interface is described by the Coulomb law. A constant value of the sliding friction coefficient *(0.8)* is assumed. The ability of this formulation to reproduce complex phenomena including sticking at the tool-chip interface due to thermal softening has been shown in [14].

2.3. Damage model

The material damage is a two steps process : the initiation of damage and its propagation (Fig. 2). Under a given load, the stress at each integration point is calculated.

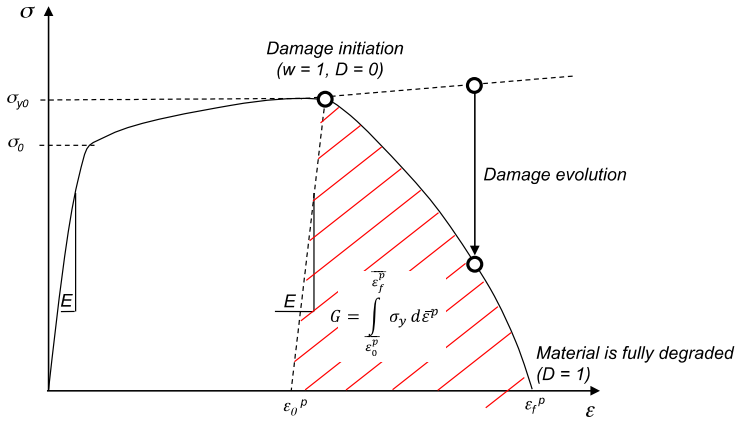

Fig. 2 : Illustration of the effects of damage on flow stress ; definition of G as the plastic strain energy.

- Damage initiation :

From $\sigma = \sigma_{y0}$ damage initiation is beginning. Indeed for each element of the numerical model, the damage W is calculated by the relation (2) :

$$W = \sum \frac{\Delta \bar{\varepsilon}^p}{\bar{\varepsilon}_0^p} \quad (2)$$

Where $\Delta \bar{\varepsilon}^p$ *is the increment of equivalent plastic,* $\bar{\varepsilon}_0^p$ the threshold equivalent plastic strain. The initiation of damage corresponds to W=1 and D=0. The threshold equivalent plastic strain at the initiation of the damage is given by the relation (3). $\bar{\varepsilon}_0^p$ is a function of the parameters D_i (i = 1 – 5) and based on the calculation of the rate of tri-axiality σ^* (first term of the equation). The second and the third terms of the equation represent respectively the sensitivity to strain rate and temperature.

$$\bar{\varepsilon}_0^p = [D_1 + D_2 \exp(D_3 \sigma^*)] \left[1 + D_4 ln \frac{\dot{\bar{\varepsilon}}}{\dot{\varepsilon}_0}\right] \left[1 - D_5 \left(\frac{T - T_0}{T_f - T_0}\right)\right] \quad (3)$$

The rate of tri-axiality is defined by $\sigma^* = \frac{\sigma_m}{\bar{\sigma}}$; σ_m is the average of the normal stresses and $\bar{\sigma}$ reprensents the von Mises equivalent stress.

- Damage propagation

After the initiation phase, the Johnson-Cook failure model permits to define the damage propagation. This last is leaded by an energetic criterion using the fracture energy G_f of the material, described by relation (4):

$$G_f = L \times G = L \int_{\bar{\varepsilon}_0^p}^{\bar{\varepsilon}_f^p} \sigma_y \, d\bar{\varepsilon}^p \quad (4)$$

where L represents the characteristic element length of the mesh (corresponding to the diagonal of the element). The determination of the energy level is crucial to reproduce the material behavior: when low energy level is implemented, the element is suppressed just after the damage onset, while high level of energy allows high deformation before total breakage.

- Fracture Energy in Ti6Al4V alloy :

In machining operations, the chip formation process is due to an intense shear in a thin zone going from the tool tip to the free surface of the chip called primary shear zone (PSZ). In the PSZ, the strain, strain rate and temperature can reach very high values. In high speeds conditions, it is not abnormal to measure strain from *3 to 6*, strain rate from 10^3 to 10^5 s^{-1}, and temperature around *600-800 K* in the primary shear zone. Therefore, fracture energy of the machined material can reach very high values. A rapid analytical calculation can give us a first approximation of the fracture energy in the chip. Indeed G can be evaluated from the flow behaviour of the material under specific conditions of strain, strain rate and temperature. For ε_p=*3,* $\dot{\varepsilon_p}$= 10^3 s^{-1} and a temperature T=*600 K* (respectively ε_p=*6,* $\dot{\varepsilon_p}$= 10^5 s^{-1} and T=*800 K*), the calculated fracture energy is G= *3000 MPa* (respectively G=*8500 MPa*).

In this paper, a parametrical study of fracture energy in the material is proposed. Numerical simulations of orthogonal cutting have been performed for a large range of fracture energy of machined material. The cutting forces and the chip morphologies are studied and discussed.

3. Numerical results and experimental validation

In this section are presented the numerical results obtained from orthogonal cutting simulation. The calculations have been performed for a feed of *0.1 mm* and a range of velocities from V=*3* to *6 m/s* (corresponding to usual cutting conditions in Ti6Al4V machining turning process). Studies of the mesh size and the material fracture energy and its effects on cutting forces and chip morphology are analyzed and discussed here in details.

3.1. Influence of mesh size

To test the numerical model response, a first analysis of mesh size influence has been realized. Calculations with element mesh size of 5, 8, 10 and *15µm* have been performed. For each calculation, the specific cutting and thrust forces (forces per unit area $\frac{F_c}{t_1.p}$ and $\frac{F_t}{t_1.p}$, respectively in the cutting and feed directions) and chip morphology were analyzed and discussed. The results of the simulations in terms of forces and time calculation are presented in Fig. 3.

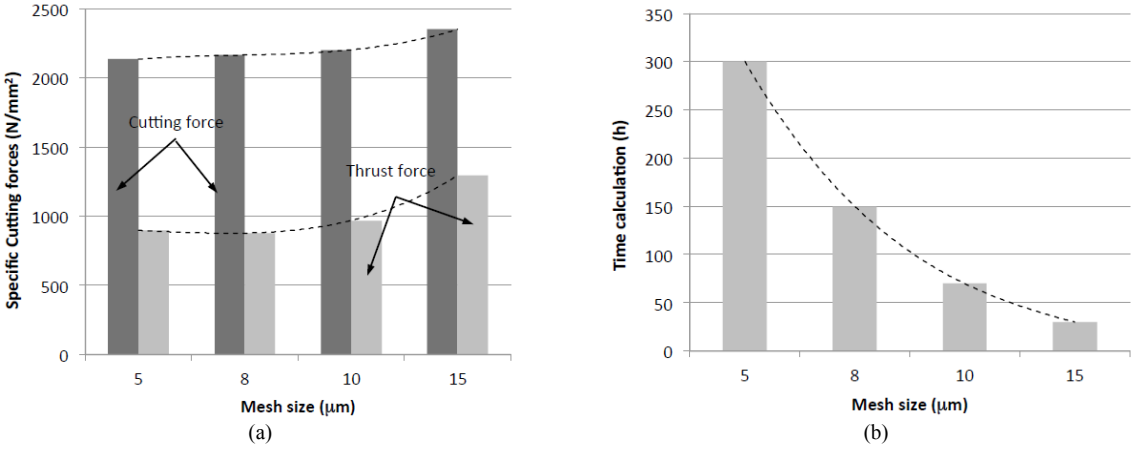

Fig. 3: Cutting and thrust forces vs element mesh size (a). Time calculation vs element mesh size (b). Simulations performed for *V=3 m/s* and $G_f = 45\ 000\ J.m^{-2}$

As observed in Fig. 3a, the specific cutting and thrust forces are maximal for the coarsest mesh (*15µm*). Both curves are slightly decreasing for the mesh size of *10* and *8µm*. From 8*µm* the cutting forces seem clearly to converge. Indeed, for this mesh size, the numerical cutting forces are $Fc=2165\ N/mm^2$ and $Ft=878\ N/mm^2$. For the smallest mesh size (*5µm*), $Fc=2135\ N/mm^2$ and $Ft=897\ N/mm^2$. Thus, the variations of the cutting forces for the both considered mesh sizes are less than 2%. In Fig. 3b, is represented the time calculation for the considered mesh sizes. As expected a coarse mesh leads to a minor computation time (around *30min* for a *15µm* mesh size). Increasing the mesh density leads clearly to higher values of time calculation: *70min* for *10µm mesh - 150min for 8µm - 300min for 5µm*. To resume, an intermediate mesh size of *8µm* offers a good compromise between time calculation (*150min* for the cutting speed *V=3m/s*) and results accuracy. This mesh density is used in the next parts of the paper.

3.2. Influence of fracture energy

As it was commented previously, the machined material can suffer extreme conditions in the primary shear zone. These conditions are leading to high values of fracture energy of the material (respectively to a lower strain at a quasi-static strain rate). Into study the effect on fracture energy on cutting forces, chip segmentation and strain at onset of shear localization, simulations were performed for a large range of G_f values (from $G_f = 15\ 000$ to $G_f = 75000\ J.m^{-2}$).

- Effect on cutting forces:

The effect of the fracture energy on the specific cutting forces is presented in Fig. 4. As expected, the value of G_f affects the level of both specific cutting and thrust forces. The first observation is that simulations performed with G_f= 15 000 J/m^2 does not show any effect of cutting speed on forces. Indeed, the low value of energy does not allow to the material to deform itself and increase its temperature due to the plastic work. Then, it can be observed that a higher value of fracture energy leads to increase the specific cutting forces (P_c increases from 1300 to 2500 N/mm^2 for respectively G_f= 15 000 and 75 000 J/m^2). Finally, the influence of the cutting speed on cutting and thrust force

presents two main trends: firstly a large decreasing of specific cutting forces for the small velocities, then a more slightly decreasing for higher values of cutting speed. The fall of forces with the velocity is due to the thermal softening of the machined material. Indeed, the first decrease of forces gets drastically more pronounced for higher values of G_f.

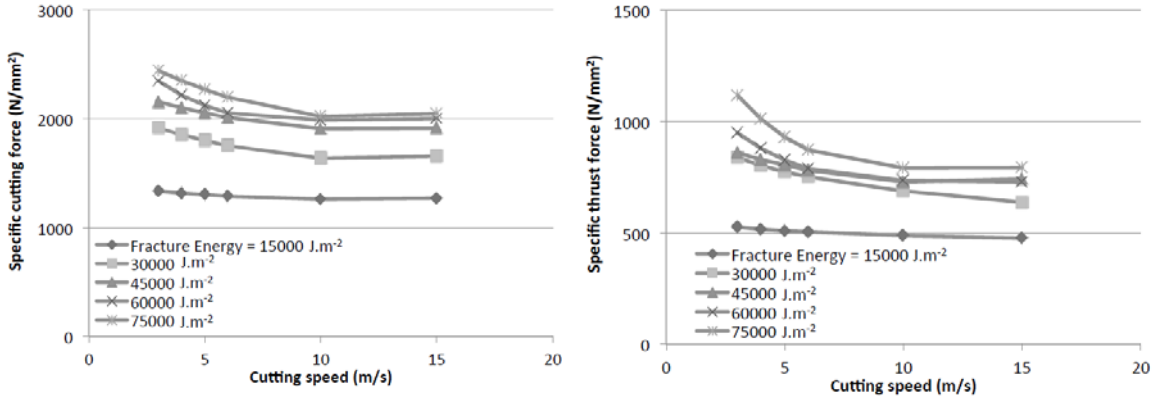

Fig. 4: Specific cutting and thrust forces in terms of cutting speed and fracture energy.

In Fig. 5 is proposed a comparison of the numerical results of specific cutting force with experimental measurements published in the literature by Molinari et al. [15] and Marino Romero [16] who performed orthogonal cutting tests on Ti6Al4V in similar cutting conditions. As observed, numerical results obteined for G_f *=30000 and 45000 J.m*$^{-2}$ give a good approximation of experimental measurements in term of specific cutting force. The decreasing of forces, in the range of considered velocities, is accurately reproduced by the numerical model.

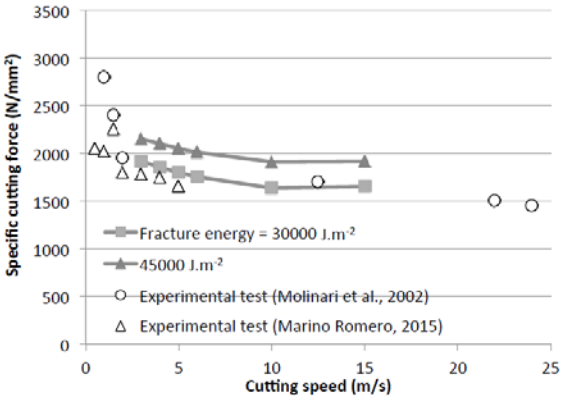

Fig. 5: Experimental vs numerical specific cutting force in function of cutting velocity for G_f =30000 and 45000 J.m^{-2}.

- Effect on chip morphology :

In Fig. 6, are presented the different chip morphologies obtained for each value of G_f (for a given value of cutting speed *V=3 m/s* and a mesh size = *8µm*). The mechanism of chip formation is highly sensitive to the level of implemented energy. Globally, increasing the fracture energy of the material has a stabilizing effect on segmentation phenomenon. Indeed, the smallest value of G_f (*15000 J/m*^{2}) leads to a complete breakage of the chip through shear banding. The shear bands are completely propagated and the material totally broken. The titanium alloy behaves as a fragile material. For G_f*=30000 J/m*^{2}, the shear bands are well defined along the chip. It can be noticed that the two firsts bands induce also a breakage of the material. Increasing the fracture energy to G_f*=45000 J/m*^{2}, the chip does

not suffer any breakage, his curvature is constant and the shear bands are perfectly defined. For highest values of G_f (*60000 and 75000 J/m*^{2}), localization of the shear (from the tool tip to the free surface of the chip) occurs but there is no clearly well defined shear band. For the highest value of energy, the deformation is less localized and the chip does not show any curvature.

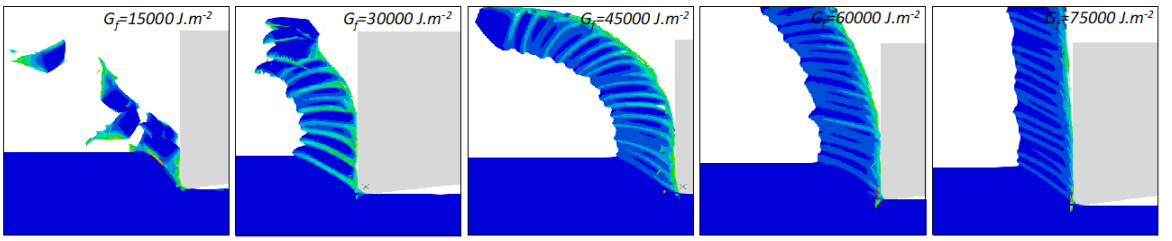

Fig. 6: Effect of fracture energy on chip morphology (*V=3m/s*, mesh size = *8μm*)

4. Conclusions

To describe the complete behavior of materials, the only constitutive law is not enough. In fact, under extreme conditions of strain, strain rates and temperature, the damage induced has to be taken into account. The paper proposes a parametrical study to determine the fracture energy of aeronautical alloy Ti6Al4V in machining processes. The analysis permits to evaluate how the chip flow behaves for different values of the fracture energy. Chip morphologies were analyzed and cutting forces compared with experimental values. A good correlation between experimental and numerical work was presented

Acknowledgements

The authors acknowledge the funding support received from the Spanish Ministry of Economy and Competitiveness and the FEDER operation program for the project “Optimización de procesos de acabado para componentes críticos de aerorreactores” (DPI2014-56137-C2-2-R).

References

[1] S. Atlati, A. Moufki, M. Nouari, B. Haddag, Tribol. Int. 105 (2017) 326–333.
[2] B. C. Schramm, H. Scheerer, H. Hoche, E. Broszeit, E. Abele, C. Berger, Surf. Coat. Technol. 188–189 (2004) 623– 629.
[3] E. Brinksmeier, W. Preuss, O. Riemer, R. Rentsch, Precis. Eng. 49 (2017) 293-304.
[4] D. Arulkirubakaran, V. Senthilkumar, Int. J. Refract. Met. Hard Mater. 62 (2017) 47–57.
[5] J. Salguero, F. Girot, M. Calamaz, M. Batista, M. Marcos, Procedia Eng. 63 (2013) 735–742.
[6] W. Lee, S.H. Kim, J. Park, B.-K. Min, J. Clean. Prod. 150 (2017) 352-360.
[7] Y. Gao, J. B. Mann, . S. Chandrasekar, R. Sun and . J. Leopold, Procedia CIRP. 58 (2017) 204 – 209..
[8] Aziz UI Hassan Mohsan, Z. Liu and G. K. Padhy, Int. J. Adv. Manuf. Technol. 91 (2017) 107–125.
[9] M. Calamaz, D. Coupard, F. Girot, Int. J. Mach. Tools Manuf. 48 (2008) 275–288.
[10] M. H. Miguélez, X. Soldani, A. Molinari, Int. J. Mater. Sci. 75 (2013) 212–222.
[11] Molinari, X. Soldani, M. H. Miguélez, J. Mech. Phys. Solid. 61 (2013) 2331-2359.
[12] G. R. Johnson, W. H. Cook, In: Proc. 7th Int. Symp. On Ballistics, Netherlands (1983) 541-547.
[13] W. S. Lee, C. F. Lin, J. Mater. Process. Technol. 75 (1998) 127–36.
[14] Molinari, R. Cheriguene, M. Miguélez, Int. J. Solids Struct. 49 (26) (2012) 3774-3796.
[15] Molinari, C. Musquar, G. Sutter, Int. J. Plast. 18 (4) (2002) 443–459.
[16] J. Marino Romero, "Formulación de un algoritmo eficiente de integración de un modelo de daño isótropo y validación en condiciones dinámicas", PhD Thesis, Carlos III de Madrid University, 2016.